

Discovery and Biological Activity of 6BrCaQ as an Inhibitor of the Hsp90 Protein Folding Machinery

Davide Audisio,^[a] Samir Messaoudi,^[a] Lukasz Cegielkowski,^[b] Jean-François Peyrat,^[a] Jean-Daniel Brion,^[a] D  lphine Methy-Gonnot,^[b] Christine Radanyi,^[b] Jack-Michel Renoir,^[b] and Mou  d Alami*^[a]

Dedicated to the memory of Dr. Christine Radanyi.

Heat shock protein 90 (Hsp90) is a significant target in the development of rational cancer therapy, due to its role at the crossroads of multiple signaling pathways associated with cell proliferation and viability. Here, a novel series of Hsp90 inhibitors containing a quinolein-2-one scaffold was synthesized and evaluated in cell proliferation assays. Results from these structure–activity relationships studies enabled identification of the simplified 3-aminoquinolein-2-one analogue **2b** (6BrCaQ),

which manifests micromolar activity against a panel of cancer cell lines. The molecular signature of Hsp90 inhibition was assessed by depletion of standard known Hsp90 client proteins. Finally, processing and activation of caspases 7, 8, and 9, and the subsequent cleavage of PARP by 6BrCaQ, suggest stimulation of apoptosis through both extrinsic and intrinsic pathways.

Introduction

Hsp90 is an emerging target of therapeutic interest for the treatment of cancer^[1] and other diseases.^[2] As a chaperone protein, Hsp90 is essential in ensuring the correct conformation, activity, intracellular localization, and proteolytic turnover for a range of proteins that are involved in cell growth, differentiation, and survival.^[3] Among 200 reported client proteins dependent upon Hsp90 machinery, 48 are directly associated with oncogenesis.^[4] Hsp90 protein functionality may be inhibited by molecules that compete with ATP binding and thereby freeze the chaperone cycle, which in turn decreases the affinity of Hsp90 for client proteins and leads to proteasome-mediated oncogenic client protein degradation. Hsp90 inhibitors block cancer cell proliferation *in vitro* and cancer growth *in vivo*.^[5] Several structurally distinct Hsp90 inhibitors, either as single agents or in combination with other cancer drugs, are currently under evaluation for anticancer activity in numerous phase II and several phase III clinical trials.^[6]

A previous hypothesis suggested the presence of two ATP binding sites on the Hsp90 protein.^[7] The N-terminal ATP binding pocket of Hsp90 is also the binding site for the structurally unrelated natural products geldanamycin (GA) and radicicol (RD) (Figure 1). The C-terminal domain has been implicated

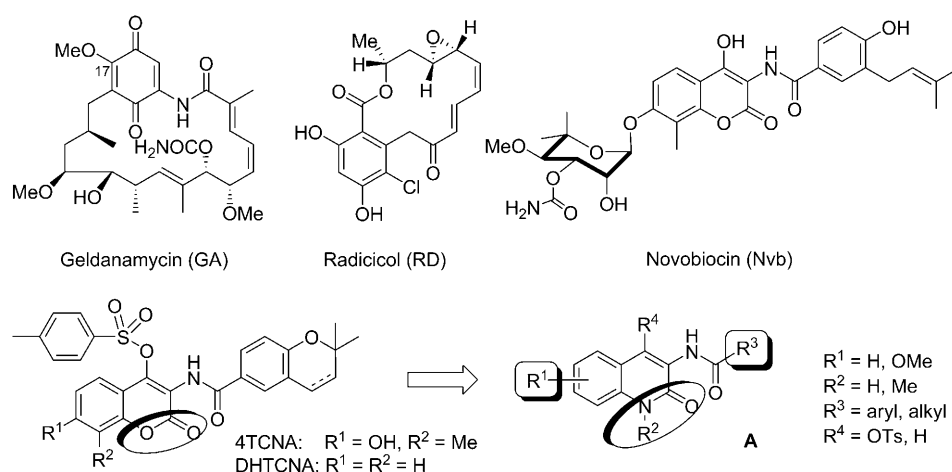


Figure 1. GA, RD, Nvb, 4TCNA, DHTCNA and general structure of the synthesized compounds A.

biochemically as the site of a possible second, cryptic, ATP binding site within Hsp90. Its contribution to the overall regulation of chaperone function is not clear, but the antibiotic no-

[a] Dr. D. Audisio, Dr. S. Messaoudi, Prof. J.-F. Peyrat, Prof. J.-D. Brion, Dr. M. Alami
Univ Paris-Sud, CNRS, BioCIS-UMR 8076
Laboratoire de Chimie Th  rapeutique, Facult   de Pharmacie
5 rue J.-B. Cl  ment, Ch  tenay-Malabry, F-92296 (France)
Fax: (+33) 1-46-83-58-28
E-mail: mouad.alami@u-psud.fr

[b] L. Cegielkowski, Dr. D. Methy-Gonnot, Dr. C. Radanyi, Dr. J.-M. Renoir
Univ Paris-Sud, CNRS, UMR 8612, Laboratoire de Pharmacologie Cellulaire et Mol  culaire des Anticanc  reux, Facult   de Pharmacie
5 rue J.-B. Cl  ment, Ch  tenay-Malabry, 92296 (France)

vobiocin (Nvb, Figure 1) has been reported to bind this site and alter the conformation of the chaperone.^[8] Although it binds with poor affinity, Nvb destabilizes Hsp90 client proteins at high concentrations (~700 μM).^[7a] A better understanding of the role of this putative Hsp90 C-domain site in regulating the function of the chaperone, as well as its potential as an anti-cancer drug target, requires further investigation. The identification of more potent site-specific inhibitors is needed and has led to the development of specific C-terminal Hsp90 inhibitors as potential anticancer therapeutics.

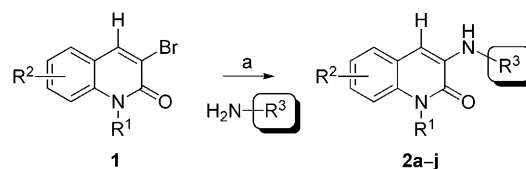
Recently, we reported a novel series of simplified 3-aminoquinolin-2(1*H*)-ones related to Nvb as a class of highly potent Hsp90 inhibitors.^[9] Removal of the noviose moiety, in addition to the introduction of a tosyl substituent at C4 of the coumarin nucleus, resulted in lead compound 4TCNA. Furthermore, we showed that removal of coumarin nucleus substituents at C7 and/or C8 is not detrimental to Hsp90 inhibitory activity (Figure 1), as DHTCNA exhibits increased inhibitory activity against the Hsp90 protein folding process.^[9b] Preliminary results regarding their mode of action reveal that these lead compounds possess Hsp90 inhibitory activity at least 15-fold higher than that of Nvb with regard to the proteasome-mediated degradation of estrogen receptor, HER2, Raf-1, and Cdk4.^[10] They also induce a high level of apoptosis in a panel of human cancer cell lines by activation of caspases and subsequent cleavage of poly(ADP-ribose) polymerase (PARP).^[11] In addition to these noteworthy pro-apoptotic properties, 4TCNA was found to mediate cell death in a p23-independent process. These results demonstrate that the simplified Nvb-like denoviose coumarins present structural originality in comparison to the already known Nvb osidic analogues.

In our continuing efforts to discover novel Hsp90 inhibitors,^[9-12] and in combination with our previous structure-activity relationship (SAR) studies, a library of quinolein-2-one derivatives was designed to probe the essential moieties of the Nvb coumarin nucleus. We proposed to construct 4TCNA and DHTCNA analogues with the coumarin core modified into a quinolein-2-one scaffold of type A (Figure 1). As coumarin isosteres, quinolein-2-ones are known to display a broad range of biological activities.^[13] Additionally, the quinolein-2-one nucleus may circumvent the low solubility of coumarin-based compounds and improve interactions in the putative ATP binding site. Furthermore, a quinolone lactame would probe the importance of hydrogen bond donors/acceptors at this position. The activity of such compounds will provide insight into interactions that are essential or that can be further optimized. The design, synthesis, and evaluation of such compounds are described in this article. Potencies of newly synthesized quinolone derivatives were evaluated using several biological assays, including cell proliferation and flow cytometry, in addition to their ability to induce proteasome-mediated degradation of HER2 (also known as ErbB2/Neu), Raf-1, Cdk4, and estrogen receptor (ER α). Among these synthetic derivatives, compound **2b** (6BrCaQ) exhibited the most potent inhibitory activity with regard to the proliferation of various cancer cells.

Results and Discussion

Chemistry

The first library of target compounds consists of simplified 3-(*N*-substituted) aminoquinolin-2(1*H*)-ones **2** without substituents at the C4 position of the heterocycle nucleus (Scheme 1). These analogues were synthesized by the palladium-catalyzed

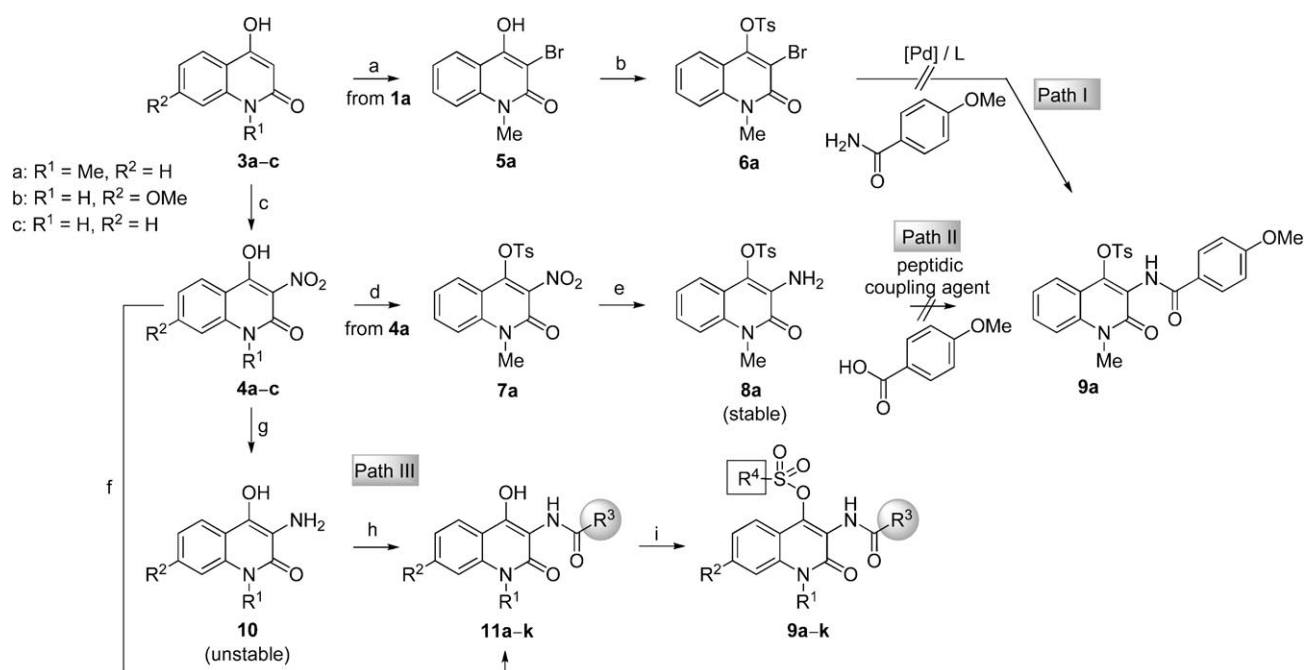


Scheme 1. Synthetic strategy to target 3-(*N*-substituted) aminoquinolin-2(1*H*)-ones **2**. Reagents and conditions: a) Pd(OAc)₂ (2.5 mol%), Xantphos (2.5 mol%), Cs₂CO₃ (2 equiv), dioxane, 100 °C, 46–95%.

C–N coupling reaction of nitrogen nucleophiles with 3-bromoquinolin-2-(1*H*)-ones **1** according to our previously reported conditions.^[14] The reactions occur rapidly in 1,4-dioxane and proceed in good to excellent yields with palladium acetate as a catalyst, xantphos as a ligand, and cesium carbonate as a base. Under these conditions, this convergent protocol provided a series of simplified aminoquinolin-2(1*H*)-ones **2a-j** with varied substituents at position 3 (Scheme 1).

Throughout the course of our studies, we decided to prepare 4TCNA and DHTCNA analogues with a quinolein-2-one scaffold of type A (R⁴ = OTs). To this end, the synthesis of quinolin-2(1*H*)-ones **9** was pursued by palladium-catalyzed coupling of 3-bromo-4-tosylquinolone **6a** with benzamides (Scheme 2, path I). All attempts to react **6a** with 4-methoxybenzamide to provide **9a** directly, using various combinations of palladium/ligand/base mixtures, were unsuccessful, likely due to steric considerations. Therefore, we decided to prepare our target compounds (**9**) under standard amide bond formation conditions, starting from the intermediate 4-tosyl-3-aminoquinolone **8a** (Scheme 2, path II). This latter compound was prepared according to a nitration^[15]/tosylation/reduction sequence from commercially available 4-hydroxyquinolone **3a**. However, the coupling reaction of **8a** to 4-methoxybenzoic acid in the presence of PyBop^[9] or EDCI^[16] failed, and starting material was recovered unchanged. We hypothesized that, through this route, the 4-tosyl substituent interfered with the outcome of the peptidic coupling.

To circumvent this drawback, an alternative synthetic pathway to the desired quinolones **9** was devised in which the peptidic coupling precedes the 4-tosylation reaction (Scheme 2, path III). This synthesis was initiated by direct reduction of the 3-nitro functionality of compound **4**, using Pd/C-catalyzed hydrogenation. The resulting amine adduct **10** is very unstable due to its photosensitivity, as was previously reported,^[17] and must be used immediately without further purification. Coupling of **10** with a series of carboxylic acid derivatives in the presence of PyBop and DIEA in DMF at room tem-



Scheme 2. Synthetic strategies to target 3-amidoquinolin-2(1*H*)-one derivatives **9**. Reagents and conditions: a) Br₂, AcOH, 74%; b) TsCl, Et₃N, CH₂Cl₂; c) AcOH, HNO₃, 88–94%; d) TsCl, Et₃N, CH₂Cl₂, 95%; e) Fe, AcOH, EtOH/H₂O (5:2), 67%; f) Onepot: 1. H₂, Pd/C, cat. HCl, THF; 2. R³COOH, PyBOP, DIPEA, 49–94% (two steps); g) H₂, Pd/C, MeOH; h) R³COOH, PyBOP, DIPEA, DMF, 13–60%; i) R⁴SO₂Cl, Et₃N, CH₂Cl₂, 70–98%.

perature gave amides **11 a–k** in low to moderate yields (13–60%).

To avoid direct manipulation and purification of the unstable coupling partner, we instead considered a one pot hydrogenation/peptidic coupling sequence, as it would be economically and environmentally advantageous over multistep synthesis. In a typical experiment, we achieved this transformation sequentially by first combining intermediate **4** with Pd/C in THF under hydrogen atmosphere. After completion, PyBop, DIEA, and aromatic or aliphatic carboxylic acids were introduced in a second step at room temperature for 12 h. We were pleased to observe that the one pot reaction worked very well using this protocol and provided the desired 3-amidoquinolones **11 a–k** in good to excellent overall yields (49–94%). Finally, synthesis of target substances **9 a–k** was achieved by tosylation reaction of intermediates **11 a–k** using tosyl chloride and triethylamine in dichloromethane as the solvent. These compounds were obtained in excellent yields (70–98%).

Biology

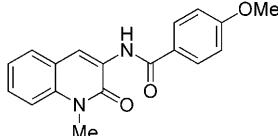
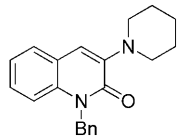
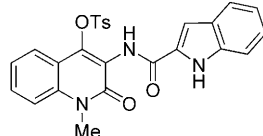
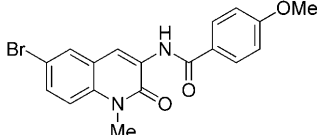
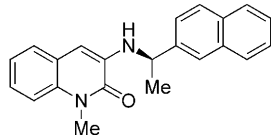
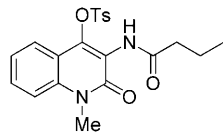
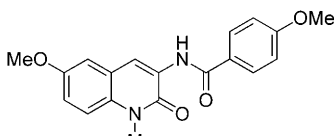
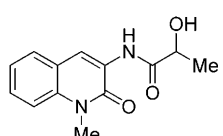
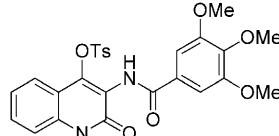
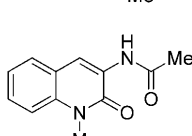
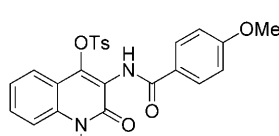
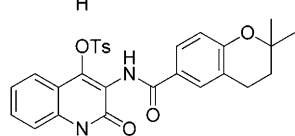
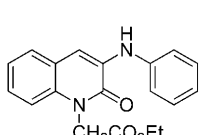
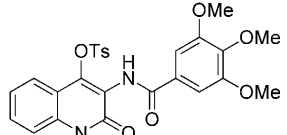
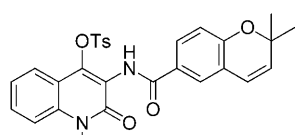
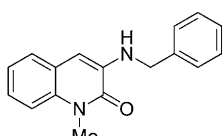
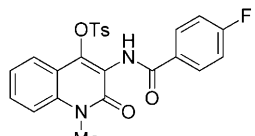
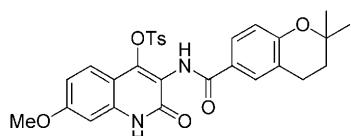
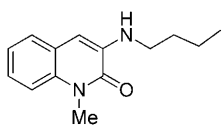
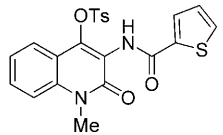
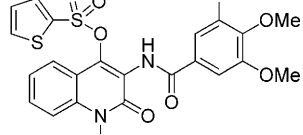
Antiproliferative activity

Upon completion of syntheses, the *in vitro* activity of quinolone derivatives **2 a–j** and **9 a–k** was evaluated by their growth inhibitory potency in MCF-7 cell line at 100 μM concentration. Quantification of cell survival was established using MTT assays after 72 h exposure (Table 1), and GI₅₀ values were determined by the concentration required to produce 50% inhibition (Table 2).

As shown in Table 1, simplified 3-(*N*-substituted) aminoquinolin-2(1*H*)-ones **2 b** and **2 c**, as well as **2 e–h**, resulted in a significant decrease (10–33%) in MCF-7 cell viability. Under exposure to **2 b** or **2 h** at 100 μM concentration, the viability of MCF-7 cells decreased to almost 10% (Table 1). Analogue **2 a** only slightly affected the growth of MCF-7 cells (89% survival) as compared to **2 b** (10% survival), clearly suggesting that the presence of a bromine atom at the C6 position of the quinolone nucleus is important for cell viability. A comparison of amide-containing analogue **2 a** with **2 f–h** revealed that introduction of an alkylamine chain at C3 of the heterocycle results in a significant decrease in MCF-7 cell viability. In contrast to analogues **2**, compounds with a tosyl group at the C4 position of the quinolone moiety exhibited only slight effects toward the growth of MCF-7 cells, and only two of these analogues, **9 i** and **9 j**, were able to decrease MCF-7 cell viability to 17–37%.

Next, growth inhibitory activities against MCF-7 breast cancer cells were measured for the selected 3-(*N*-substituted) aminoquinolin-2(1*H*)-ones. All of the compounds shown in Table 2 are more potent cell growth inhibitors in comparison to Nvb, except for **9 f**, which has an aliphatic amide chain. 4-Tosylquinolone analogue **9 e**, with a 2-indole carboxamide side chain, exhibited approximately twofold greater growth inhibition activity than that of **9 i**, which in turn is nearly fourfold more active than Nvb. Interestingly, **9 j**, which has a free quinolone lactame, displays potent growth inhibitory activity at the micromolar level (GI₅₀ = 8 μM), suggesting that activity increases as hydrogen bond donor/acceptor properties of the inhibitor increases. Of the six selected C4-unsubstituted quinolone derivatives, **2 b** and **2 c** demonstrated significant ability to in-

Table 1. Antiproliferative effect of **2a–j** and **9a–k** derivatives against MCF-7 cells.

Compd	Viability ^[a] [%]	Compd	Viability ^[a] [%]	Compd	Viability ^[a] [%]
	89		12		50
	10		51		50
	22		96		55
	90		82		112
	33		84		37
	32		57		17
	20		65		77

[a] Value of the anti-proliferative effect (% of viable cells compared to untreated cells 100%) of analogues **2a–j** and **9a–k** in MCF-7 cells at 100 μM concentration.

hibit cell growth. Compound **2b** (6-bromo-3-[4-methoxyphenylcarbamoyl]-quinolin-2-one, 6BrCaQ) was the most cytotoxic against the MCF-7 cell line.

Next, 6BrCaQ was evaluated for its cytotoxic activity against six other cancer cell lines, including human ductal breast epithelial cancer (T47D), human ovarian cancer (IRGOV-1), endometrial cancer (Ishikawa), human colon cancer (HT-29 and Caco-2), and human breast cancer (MDA-MB231). The results of this study, summarized in Table 3, revealed that compound 6BrCaQ inhibited the growth of all tested tumor cell lines, with GI_{50} values ranging from 2 to 32 μM , and this effect was not dependent on cell type. The Ishikawa endometrial and MDA-MB231 ER-negative breast cancer cell lines were significantly more sensitive ($\text{GI}_{50} \sim 2\text{--}3 \mu\text{M}$), while the HT-29 colon cancer cell line was less responsive ($\text{GI}_{50} = 32 \mu\text{M}$), to growth inhibition

by 6BrCaQ. In comparison, 4TCNA and Nvb exerted significantly less ability to inhibit proliferation of all cell lines, with GI_{50} values ranging from 43 to 62 and from 115 to 475 μM , respectively. Consequently, the quinolone scaffold appears to be a suitable replacement for the coumarin core in this series with regard to antiproliferative activity.

Proteasome-mediated ER α degradation

In order to confirm that the growth inhibitory activity displayed by these quinolinone derivatives was a consequence of Hsp90 inhibition, the most cytotoxic compounds, 6BrCaQ and **9j**, were incubated with MCF-7 cells (24 h at 100 μM), then the cell extracts were subjected to Western blot analyses. Given that inhibition of Hsp90 leads to proteasome-mediated degra-

Table 2. Antiproliferative effects of selected compounds 2 and 9 in MCF-7 human breast cancer cells.	
Compd	GI ₅₀ [μ M] (MCF-7) ^[a]
2b (6BrCaQ)	7
2c	10
2e	18
2f	60
2g	27
2h	45
9e	30
9f	100
9i	70
9j	8
DHTCNA	35
4TCNA	50
Novobiocin	260

[a] GI₅₀ = concentration of compound needed to reduce cell growth by 50% following 72 h cell treatment with the tested drug (average of three experiments). Values are the mean of two independent experiments in which no more than 5.5 variations were measured.

Table 3. Cytotoxic activity of selected compounds 6BrCaQ, 4TCNA, and Nvb.			
	6BrCaQ	GI ₅₀ [μ M] ^[a] 4TCNA	Nvb
MCF-7 ^[b]	7	50	260
T47D ^[b]	15	40	115
IGROV-1 ^[b]	5	43	360
Ishiwaka ^[b]	2	50	300
HT-29 ^[b]	32	45	150
MDA-MB-231 ^[b]	2	45	220
Caco-2 ^[b]	8	62	475

[a] GI₅₀ = concentration of compound needed to reduce cell growth by 50% following 72 h cell treatment with the tested drug (average of three experiments). [b] T47D = human ductal breast epithelial cancer; IRGOV-1 = human ovarian cancer; Ishiwaka = endometrial cancer; HT-29 and Caco-2 = human colon cancer; MCF-7 = human breast cancer, and MDA-MB-231 = hormone-independent breast cancer. [c] GI₅₀ values for 4TCNA and Nvb were determined in this study.

dation of client proteins, we first questioned if the selected compounds could affect the stability of the transcription factor ER, which is a Hsp90 client protein. As shown in Figure 2a, quinolones 6BrCaQ and **9j** are able to induce proteasome-mediated loss of ER α protein, suggesting inhibition of Hsp90 and disruption of heteroprotein complexes. The activity of these two compounds was inhibited by proteasome inhibitor MG-132. Notably, analogues **2c**, **2e**, **2g**, and **9e**, which displayed GI₅₀ values of 10 to 30 μ M (Table 2), proved to be inactive with regard to proteasome-mediated ER α degradation (data not shown). These data suggest that these analogues may selectively affect different Hsp90/client protein complexes than do 4TCNA and DHTCNA. In dose-response analysis (shown in Figure 2b), compounds 6BrCaQ and **9j** both induced concentration-dependent degradation of Hsp90 client protein ER α . The antiproliferative activities (6BrCaQ, GI₅₀ = 7 μ M; **9j**, GI₅₀ = 8 μ M) correlate well to the concentrations needed to induce Hsp90 client protein degradation, directly linking Hsp90 inhibition to cell viability.

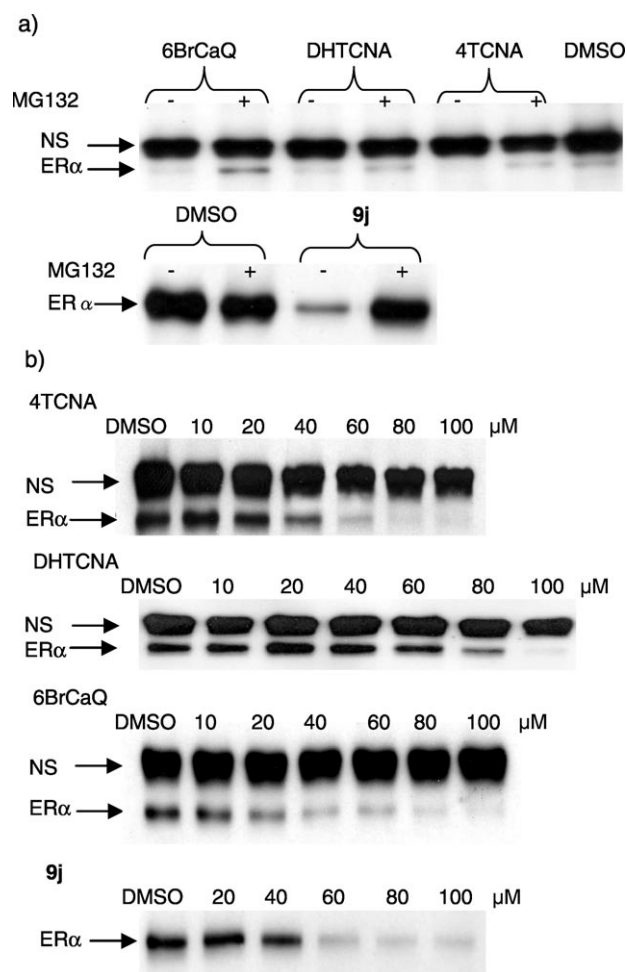


Figure 2. a) Effects of quinolone analogues 6BrCaQ, **9j**, 4TCNA, and DHTCNA on ER α stability. MCF-7 cells were grown and exposed to 100 μ M Hsp90 inhibitors 6BrCaQ, **9j**, 4TCNA, and DHTCNA as described in the Experimental Section in the presence (+) or absence (-) of proteasome inhibitor MG132 (5 μ M) for 24 h, and cell lysates were analyzed by Western blotting with regard to levels of ER α . DMSO was used as a control; NS = nonspecific protein band detected under these conditions which served as a control for constant protein loading; b) Dose-response of ER α fate following exposure of MCF-7 cells to increasing concentrations of 6BrCaQ and **9j** for 16 h. Cells were cultured and treated, with cell lysates analyzed as above.

To provide additional evidence that the growth inhibitory activity manifested by 6BrCaQ and **9j** resulted from Hsp90 inhibition, 6BrCaQ and **9j** were evaluated for their ability to induce degradation of other Hsp90-dependent client proteins, including Her2, Raf-1, and Cdk4, the most widely studied molecular signatures indicative of Hsp90 blockade. As depicted in Figure 3a, exposure to 6BrCaQ resulted in degradation of Her2, Cdk4, and Raf-1 at levels similar to 4TCNA treatment. The non-Hsp90-dependent protein NS was not affected by 6BrCaQ, indicating selective degradation of Hsp90-dependent clients. Expression of Raf-1, a key signalling protein in the Ras-MAP kinase pathway, was affected to a greater extent by 6BrCaQ in a concentration-dependent manner as compared to 4TCNA (Figure 3b). Raf-1 levels were significantly decreased at relatively low concentrations of 6BrCaQ (~7 μ M, Figure 3c). The

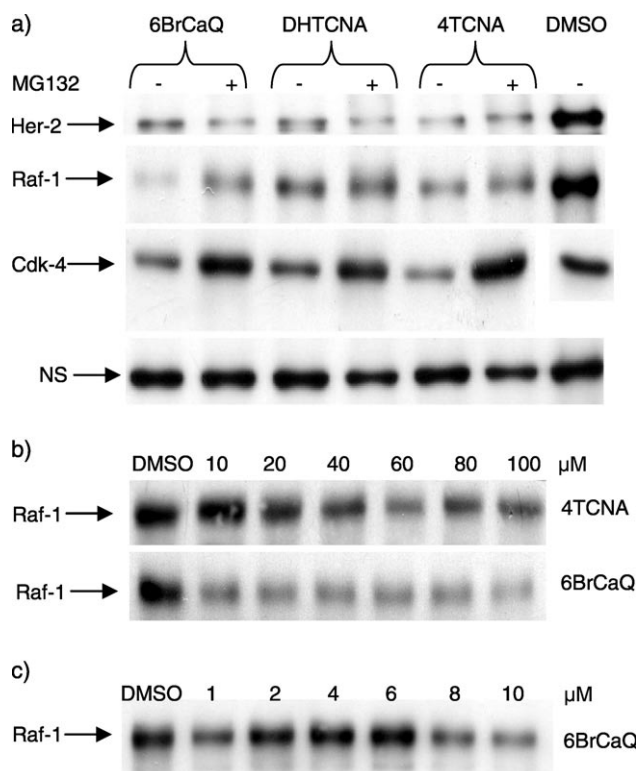


Figure 3. a) Western blot analysis of Hsp90-dependent client proteins Her-2, Raf-1, and Cdk-4 from MCF-7 breast cancer cell lysates upon treatment with 100 μM 6BrCaQ in the presence (+) or absence (–) of MG132 (5 μM). DMSO was used as a control. NS = nonspecific protein that served as an internal loading control; b) Dose–response of Raf-1 fate following exposure of MCF-7 cells to increasing concentrations of 6BrCaQ for 16 h. Cells were cultured and treated, with cell lysates analyzed by Western blotting with regard to Raf-1 levels.

anti-proliferative activity of 6BrCaQ ($\text{IC}_{50} = 7 \mu\text{M}$, Table 2) correlates well to the concentration needed to induce Hsp90/Raf-1 client protein degradation. These data suggest that 6BrCaQ may exhibit a different affinity and mechanism of action towards various Hsp90/client protein complexes. Overall, these results are in agreement with previous studies showing that the various client protein kinases are not equally responsive to Hsp90 inhibitors, and that sensitivity may depend on the interaction of each kinase interacts with Hsp90 and the cochaperone cdc37.^[18]

Upon comparison with 6BrCaQ, it was surprising to note that the compound exhibiting the second highest cytotoxicity, **9j**, does not induce any degradation of client proteins Her2, Cdk4, and Raf-1 (data not shown), suggesting that **9j** exhibits its biological activity through a different mode of action than was previously described for compounds 6BrCaQ, 4TCNA, and DHTCNA. Importantly, 6BrCaQ and compound **9j** can be considered compounds which affect various clusters of Hsp90 client proteins as suggested for celastrol, which preferentially affects the Hsp90–cdc37 interaction.^[19]

Table 4. Flow cytometry analysis of MCF-7 cells treated with analogue 6BrCaQ (100 μM) for 48 h and 72 h.^[a]

Compd	SubG ₁		G ₂ /M [%] 48 h
	48 h	72 h	
DMSO	7.4	4.5	13.4
4TCNA	28.8	43.2	20.6
6BrCaQ	29.5	47.0	48.0

[a] Data represent percentage of cells in subG₁ and G₂/M phases of the cell cycle. Values are the mean of two independent experiments in which no more than 2.5 variations were measured.

Flow cytometry analysis

Cell cycle arrest was assessed in MCF-7 cancer cells following 6BrCaQ treatment for 48 h and 72 h. As shown in Table 4, treatment with 6BrCaQ at a concentration of 100 μM affected cell cycle progression of MCF-7 cells, and resulted in cell cycle arrest in the G₂/M phase, similarly to 4TCNA. The subG₁ phase, which represents apoptotic or necrotic cells, was found to be significantly increased upon 6BrCaQ exposure as compared to the control (29.5% versus 7.4%, respectively). Prolonged incubation with compound 6BrCaQ (72 h) increases the subG₁ phase to 47% without further changes in G₂/M phase as compared to 48 h treatment. These data reveal that 6BrCaQ is a more potent inducer of G₂/M arrest and apoptosis in MCF-7 cell line than 4TCNA.

Caspase involvement in 6BrCaQ-induced apoptosis of MCF-7 cells and PARP cleavage

In light of the finding that 6BrCaQ potentially induced apoptosis, we next investigated the extent to which this effect involved extrinsic or intrinsic pathways. Apoptosis can be initiated by various means, such as stimulation of cell surface death receptors upon specific ligand or antibody binding (extrinsic pathway), perturbation of mitochondrial function (intrinsic pathway), or triggering by autoactivation of initiator caspases (e.g., 8 and 9), which in turn activate effector caspases (e.g., 3 and 7).^[20] Although MCF-7 cells lack procaspase 3,^[21] Liang et al. showed that in these cells, the apoptotic pathway was able to proceed via sequential activation of caspase 9, followed by that of caspases 7 and 6.^[22] Since caspase 7 can be activated by both intrinsic and extrinsic apoptotic pathways, we analyzed processing of caspases 9 and 8, respectively. Upon exposure of MCF-7 cells to 6BrCaQ, cleavage of poly(ADP-ribose) polymerase (PARP), a marker of mitochondrial apoptosis, was detected as early as 24 h and gradually increased after 48 h and 72 h of treatment (Figure 4b). Consequently, activation of caspase 7, responsible for PARP cleavage in MCF-7 cells, was observed to progress throughout the 72 h exposure to 6BrCaQ (A1, Figure 4a). Moreover, activation of caspases 8 and 9, detected in 6BrCaQ treated samples, indicated that apoptosis was triggered through intrinsic and extrinsic pathways (A2 and A3, Figure 4a). This result differentiates 6BrCaQ from reference compound 4TCNA, which was found to initiate only the extrinsic pathway of apoptosis through caspase 8.^[9a] Thus, 6BrCaQ

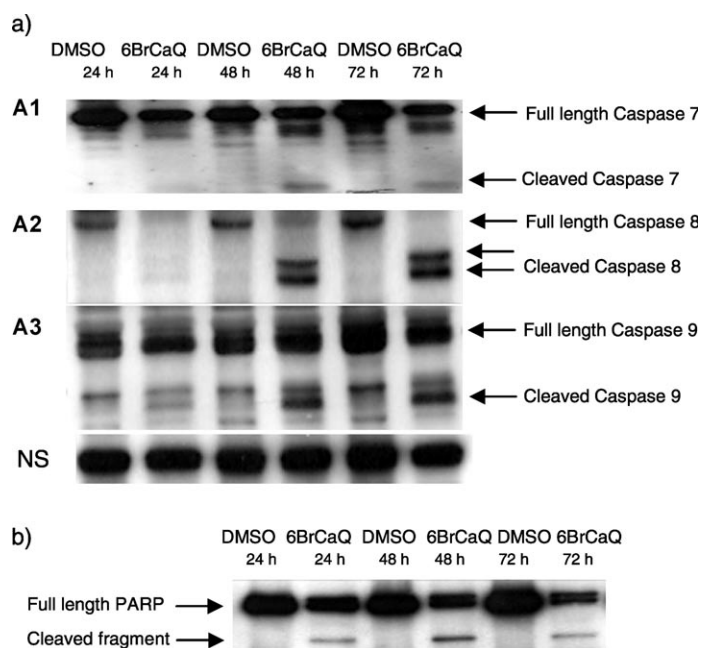


Figure 4. Effects of 6BrCaQ on caspase activation and PARP cleavage. a) MCF-7 cells were cultured overnight with DMSO or 100 μM compound 6BrCaQ, and cell lysates (20 μg protein) were fractionated by SDS-PAGE (12% acrylamide) followed by Western blotting. DMSO was used as a control. NS = nonspecific protein that served as an internal loading control; b) PARP cleavage following exposure of MCF-7 cells to 6BrCaQ for 16 h. Cell lysates were analyzed by SDS-PAGE (8% acrylamide) and subjected to Western blot analysis using an anti-PARP antibody.

appears to be a more potent inducer of apoptosis than 4TCNA.

As we established that 6BrCaQ promotes apoptosis through activation of caspases and subsequent cleavage of PARP, we next questioned whether 6BrCaQ also affects the expression of p23, which may be associated with apoptosis.^[23] Indeed, the cochaperone p23 associates with Hsp90 in complexes containing client proteins (i. e., steroid receptors), different from those

in which the cochaperone cdc37 is found (i. e., oncogenic kinases). In addition, association with Hsp90 protects p23 from cleavage.^[23c] As illustrated in Figure 5A, exposure of MCF-7 cells to 6BrCaQ induced cleavage of Hsp90-associated p23. This activity may be crucial for Hsp90 inhibition, since p23 was recently reported to exert a protective effect against Hsp90 inhibitors.^[24] Moreover, targeting p23 in addition to Hsp90 may be beneficial for a vast majority of human malignancies that express telomerase.^[25]

Finally, we were interested in determining the effect of 6BrCaQ in the autophagy process. Autophagy is involved in programmed cell death (PCD) II, which is characterized by the accumulation of autophagic vesicles (autophagosomes and autophagolysosomes) and is often observed when massive cell elimination is required or when phagocytes do not have easy access to dying cells. A recent study suggests that autophagy may cause cell death.^[26] Caspase inhibitor-induced autophagic cell death is severely affected by RNA interference (RNAi) involving expression of ATG7 and beclin 1, two genes whose products are essential for autophagy.^[27] Moreover, it may assist in preventing or halting the progression of some diseases, such as various types of neurodegeneration and cancer.^[26]

MCF-7 cells were treated with compound 6BrCaQ at a concentration of 100 μM , and Western blot analysis revealed that 6BrCaQ led to significant increases in the ratio of autophagosomal markers LC3II/LC3I (Figure 5b). The expression of LC3II gradually increased over the duration of treatment. From these results, we conclude that 6BrCaQ can indeed induce an autophagic process. Whether this process orients cells toward survival or apoptosis is under current investigation, but preliminary results (not shown) suggest that 6BrCaQ may trigger cell death through a number of pathways in which autophagy has a prominent role.

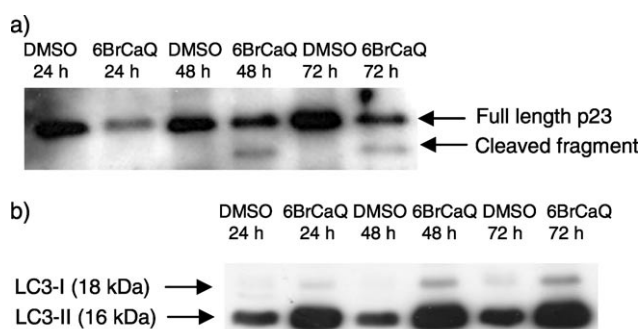


Figure 5. a) Effect of 6BrCaQ on the expression of p23 in MCF-7 cancer cells. MCF-7 cells were cultured with DMSO or compound 6BrCaQ (100 μM) for 24 h, and cell lysates (10 μg protein) were fractionated by SDS-PAGE (12% acrylamide) and subjected to Western blot analysis using a JJ3 antibody. DMSO was used as a control. NS = nonspecific protein that served as an internal loading control; b) Effect of 6BrCaQ on the expression of autophagy-linked proteins by Western blot. LC3I = cytoplasmic form of autophagosome marker LC3; LC3II = form associated with the autophagosome.

Conclusions

In summary, we have synthesized and biologically evaluated a new series of 3-(N-substituted)aminoquinolin-2(1H)-one derivatives. From these SAR studies, 6BrCaQ was found to display the most potent antiproliferative activity against a panel of cancer cell lines and to manifest downregulation of several Hsp90 client proteins. Moreover, 6BrCaQ induced a high level of apoptosis in MCF-7 breast cancer cells by activation of caspases and the subsequent cleavage of PARP. In addition to these noteworthy pro-apoptotic properties, only 6BrCaQ, in contrast to **9j**, was found to mediate cell death in a p23-independent process. Together, these data suggest that compounds from this family of Hsp90 inhibitors may target different clusters of Hsp90 client proteins.

Experimental Section

Chemistry

Melting points (mp) were recorded on a Büchi B-450 apparatus and are uncorrected. NMR spectra were collected on a Bruker AMX 200 (^1H , 200 MHz; ^{13}C , 50 MHz), Bruker AVANCE 300, or Bruker AVANCE 400 (^1H , 400 MHz; ^{13}C , 100 MHz). Unless otherwise stated, CDCl_3 was used as a solvent. Chemical shifts (δ) are reported in parts per million (ppm), and the following abbreviations are used: singlet (s), doublet (d), triplet (t), multiplet (m), quintet (q), broad doublet (bd), broad multiplet (bm), broad triplet (bt), and broad singlet (bs). Elemental analyses (C, H, N) were performed by the microanalyses service of the Faculty of Pharmacy at Châtenay-Malabry (France) and were within 0.4% of the theoretical values otherwise stated. Mass spectra were obtained using a Bruker Esquire electrospray ionization apparatus.

Materials: DMF distilled from BaO, CH_2Cl_2 distilled from CaH_2 , and usual solvents were purchased from SDS (Paris, France). Liquid chromatography was performed on Merck silica gel 60 (70/30 mesh), and TLC was performed on silica gel, 60F-254 (0.26 mm thickness) plates. Visualisation was achieved with UV light and phosphomolybdic acid reagent unless otherwise stated. Proteasome inhibitor MG132 was obtained from Sigma and used at 5 μM concentration. All other reagents were of high grade and were used without further purification. Analogues **2a–j** were prepared according to our previously reported procedure.^[14b]

Preparation of compound 3b: POCl_3 (14 mL) was added dropwise to a suspension of 3-anisidine (8 mL, 71 mmol) and malonic acid (7.4 g, 71 mmol). The suspension was heated for 1–2 h to 100 °C, then the mixture was poured into ice/water, and the precipitate was filtered, dissolved in aq NaOH (2 N), and filtered again. The solution was acidified with HCl (2 N), filtered by suction, washed with water, and dried to give a 4:1 mixture of the 5-methoxy- and 7-methoxy-4-quinolone isomers. The crude residue was purified with difficulty by column chromatography on silica gel ($\text{CH}_2\text{Cl}_2/\text{MeOH}$, 95:5) to yield desired quinolone **3b** as a beige solid (5.5 g, 40%); $R_f=0.35$ ($\text{CH}_2\text{Cl}_2/\text{MeOH}$, 95:5); mp: > 300 °C (Lit.: > 300 °C); ^1H NMR (300 MHz, $[\text{D}_6]\text{DMSO}$): $\delta=11.18$ (bs, 1H), 11.03 (s, 1H), 7.67 (d, 1H, $J=8.8$ Hz), 6.76–6.72 (m, 2H), 5.58 (s, 1H), 3.79 ppm (s, 3H); ^{13}C NMR (75 MHz, $[\text{D}_6]\text{DMSO}$): $\delta=163.8$, 162.5, 161.3, 140.9, 124.1, 109.7, 108.7, 97.8, 95.8, 55.2 ppm; IR (neat): $\tilde{\nu}=2921$, 1669, 1628, 1603, 1553, 1509, 1468, 1437, 1381, 1330, 1264, 1247, 1232, 1215, 1184, 1151, 1094, 1016, 862, 829, 804, 733, 632, 594, 579 cm^{-1} ; MS (APCI+): m/z : 192.0 $[\text{M}+\text{H}]^+$.

General protocol for nitration: HNO_3 (70%, 9 mmol) was added dropwise to a suspension of 4-hydroxyquinolin-2(1H)-one **1** (6 mmol) in glacial acetic acid (10 mL). The mixture was heated at 90 °C for 1–2 h, then cooled to RT. The solid was collected by filtration and thoroughly washed with Et_2O .

Compound 4a: Yellow solid (1.76 g, 93%); $R_f=0.28$ ($\text{CH}_2\text{Cl}_2/\text{MeOH}$, 8:2); mp: 158–160 °C (Lit.: 159–161 °C); ^1H NMR (300 MHz, $[\text{D}_6]\text{DMSO}/\text{CD}_3\text{OD}$): $\delta=8.12$ (dd, 1H, $J_1=8.1$ Hz, $J_2=1.4$ Hz), 7.76 (t, 1H, $J=8.4$ Hz), 7.57 (d, 1H, $J=8.5$ Hz), 7.38 (t, 1H, $J=7.6$ Hz), 3.60 ppm (s, 3H); ^{13}C NMR (75 MHz, $[\text{D}_6]\text{DMSO}/\text{CD}_3\text{OD}$): $\delta=155.3$, 154.1, 138.9, 133.4, 127.1, 124.8, 122.5, 115.2, 114.5, 29.2 ppm; IR (neat): $\tilde{\nu}=1663$, 1617, 1590, 1525, 1418, 1196, 867, 763, 662, 576, 564 cm^{-1} ; MS (APCI+): m/z : 221.2 $[\text{M}+\text{H}]^+$.

Compound 4b: Orange solid (450 mg, 73%); $R_f=0.34$ ($\text{CH}_2\text{Cl}_2/\text{MeOH}$, 8:2); ^1H NMR (300 MHz, $[\text{D}_6]\text{DMSO}$): $\delta=11.80$ (s, 1H), 7.94 (d, 1H, $J=9.0$ Hz), 6.89 (dd, 1H, $J_1=9.0$ Hz, $J_2=2.2$ Hz), 6.78 (d, 1H,

$J=2.2$ Hz), 3.83 ppm (s, 3H); ^{13}C NMR (75 MHz, $[\text{D}_6]\text{DMSO}$): $\delta=163.3$, 157.5, 155.9, 140.4, 126.3, 125.1, 111.6, 107.2, 98.1, 55.5 ppm; IR (neat): $\tilde{\nu}=2845$, 1670, 1597, 1520, 1478, 1429, 1395, 1319, 1268, 1248, 1222, 1192, 1159, 1108, 1016, 968, 836, 813, 785, 693, 661, 640 cm^{-1} ; MS (APCI+): m/z : 237.2 $[\text{M}+\text{H}]^+$.

Compound 4c: Orange solid (1.07 g, 42%); $R_f=0.16$ ($\text{CH}_2\text{Cl}_2/\text{MeOH}$, 8:2); mp: 236–238 °C (Lit.: 216 °C); ^1H NMR (300 MHz, $[\text{D}_6]\text{DMSO}$): $\delta=12.00$ (bs, 1H), 10.96 (bs, 1H), 8.05 (d, 1H, $J=8.0$ Hz), 7.67 (t, 1H, $J=7.4$ Hz), 7.35 (d, 1H, $J=8.3$ Hz), 7.30 ppm (t, 1H, $J=7.7$ Hz); ^{13}C NMR (75 MHz, $[\text{D}_6]\text{DMSO}$): $\delta=156.3$, 155.7, 138.0, 133.0, 127.1, 124.4, 122.2, 115.8, 114.0 ppm; IR (neat): $\tilde{\nu}=2847$, 1667, 1605, 1525, 1480, 1438, 1411, 1186, 1165, 1145, 1114, 1027, 891, 790, 764, 753, 666, 613 cm^{-1} ; MS (APCI–): m/z : 204.9 $[\text{M}–\text{H}]^+$.

Preparation of compound 8a: A stirred suspension of **7a** (930 mg, 2.48 mmol) and Fe powder (1.2 g, 21 mmol) in a mixture of EtOH (10 mL), acetic acid (10 mL), water (4 mL), and HCl (37%, 5 drops) was stirred vigorously at reflux. After 2.5 h, the reaction mixture was cooled and filtered through Celite. The filtrate was diluted with saturated aq NaHCO_3 and extracted with CH_2Cl_2 (3×10 mL). The combined organic layers were dried over Na_2SO_4 and evaporated, and the residue was further purified by flash chromatography to yield the desired 4-tosyl-3-aminoquinolone **8a** as a white solid (570 mg, 67%); $R_f=0.53$ ($\text{CH}_2\text{Cl}_2/\text{EtOAc}$, 95:5); mp: 127–129 °C; ^1H NMR (300 MHz, CDCl_3): $\delta=7.85$ (d, 2H, $J=8.2$ Hz), 7.38–7.16 (m, 5H), 7.05 (td, 1H, $J_1=8.0$ Hz), 4.65 (bs, 2H), 3.68 (s, 3H), 2.38 ppm (s, 3H); ^{13}C NMR (75 MHz, $[\text{D}_6]\text{DMSO}$): $\delta=158.2$, 146.1, 132.4, 131.6, 130.3 (2C), 129.9, 128.2 (2C), 127.6, 125.9, 122.5, 119.9, 117.9, 114.5, 30.1, 21.2 ppm; IR (neat): $\tilde{\nu}=3455$, 3338, 1621, 1589, 1468, 1418, 1349, 1306, 1259, 1194, 1178, 1124, 1091, 1055, 1007, 847, 814, 772, 746, 732, 700, 666, 633, 617, 593 cm^{-1} ; MS (APCI+): m/z : 345.0 $[\text{M}+\text{H}]^+$.

General protocol for one pot amide formation: A round-bottomed flask, protected from light by an aluminium sheet, was charged with 10% Pd/C (110 mg), 4-hydroxy-3-nitroquinolone **4** (1 mmol), concd HCl (12 N, few drops), and freshly distilled dry THF (7 mL). The flask was sealed and purged with three vacuum/nitrogen cycles. The vacuum outlet was then replaced with two hydrogen balloons, and the reaction was stirred at RT for 8 h until completion, as determined by TLC. Next, DIPEA (10 equiv) was added dropwise under nitrogen atmosphere. The coupling agent PyBOP (1.2 mmol) and the appropriate acid (1.2 mmol) were added portionwise. This operation was done under protection from light. After the mixture stirred for 12 h at RT, EtOAc was added, and the combined organic layers were filtered through a plug of Celite, flushing with EtOAc. After concentration under vacuum, the organic layer was washed once with aqueous HCl (1 M) and twice with brine, dried over Na_2SO_4 , and concentrated under vacuum. The crude residue was purified by column chromatography on silica gel to yield the corresponding amide **11a–i**.

Compound 11a: Yellow solid (133 mg, 60%); $R_f=0.34$ (cyclohexane/EtOAc, 6:4); mp: 197–199 °C; ^1H NMR (300 MHz, CDCl_3): $\delta=13.28$ (s, 1H), 9.47 (s, 1H), 8.19 (dd, 1H, $J_1=8.0$ Hz, $J_2=1.5$ Hz), 7.96 (d, 2H, $J=8.9$ Hz), 7.57 (ddd, 1H, $J_1=8.6$ Hz, $J_2=7.2$ Hz, $J_3=1.5$ Hz), 7.35–7.29 (m, 2H), 6.92 (d, 2H, $J=8.9$ Hz), 3.81 (s, 3H), 3.70 ppm (s, 3H); ^{13}C NMR (75 MHz, CDCl_3): $\delta=166.2$, 163.3, 159.9, 148.8, 136.6, 130.3, 129.6 (2C), 124.7, 124.4, 122.6, 117.4, 114.2 (2C), 113.7, 109.4, 55.5, 30.0 ppm; IR (neat): $\tilde{\nu}=3321$, 2927, 1736, 1644, 1591, 1568, 1534, 1499, 1464, 1415, 1375, 1356, 1312, 1258, 1178, 1120, 1089, 1027, 897, 838, 749, 673, 651, 613, 581, 557 cm^{-1} ; MS (APCI+): m/z : 325.1 $[\text{M}+\text{H}]^+$.

Compound 11b: Pale yellow solid (157 mg, 60%); $R_f=0.41$ ($\text{CH}_2\text{Cl}_2/\text{EtOAc}$, 9:1); mp: 184–186 °C; $^1\text{H NMR}$ (300 MHz, CDCl_3): $\delta=13.01$ (s, 1H), 9.39 (s, 1H), 8.09 (d, 1H, $J=8.3$ Hz), 7.48 (t, 1H, $J=8.3$ Hz), 7.30–7.17 (m, 2H), 7.11 (s, 2H), 3.88 (s, 6H), 3.85 (s, 3H), 3.67 ppm (s, 3H); $^{13}\text{C NMR}$ (75 MHz, CDCl_3): $\delta=166.4$, 159.9, 153.5 (2C), 149.0, 142.2, 136.7, 130.6, 127.5, 124.8, 122.8, 117.4, 113.8, 109.3, 105.0 (2C), 61.1, 56.5 (2C), 30.1 ppm; IR (neat): $\tilde{\nu}=3325$, 2927, 1650, 1611, 1585, 1537, 1499, 1461, 1415, 1376, 1360, 1339, 1234, 1182, 1128, 1093, 1006, 910, 848, 775, 751, 679, 655, 632, 579, 566 cm^{-1} ; MS (ESI+): m/z : 407.4 $[\text{M}+\text{Na}]^+$.

Compound 11c: White solid (200 mg, 94%); $R_f=0.59$ (cyclohexane/EtOAc, 6:4); mp: 189–191 °C; $^1\text{H NMR}$ (300 MHz, CDCl_3): $\delta=13.02$ (s, 1H), 9.52 (s, 1H), 8.18 (dd, 1H, $J_1=8.0$ Hz, $J_2=1.5$ Hz), 8.01 (dd, 2H, $J_1=8.8$ Hz, $J_2=5.2$ Hz), 7.57 (ddd, 1H, $J_1=8.5$ Hz, $J_2=7.2$ Hz, $J_3=1.5$ Hz), 7.34 (d, 1H, $J=8.5$ Hz), 7.32 (t, 1H, $J=7.6$ Hz), 7.19 (t, 2H, $J=8.5$ Hz), 3.76 ppm (s, 3H); $^{13}\text{C NMR}$ (75 MHz, CDCl_3): $\delta=165.6$, 165.5 (d, 1C, $J_{\text{CF}}=254.6$ Hz), 159.7, 148.9, 136.6, 130.5, 130.1 (d, 2C, $J_{\text{CF}}=9.2$ Hz), 128.4 (d, 1C, $J_{\text{CF}}=2.3$ Hz), 124.7, 122.7, 117.2, 116.1 (d, 2C, $J_{\text{CF}}=22.1$ Hz), 113.7, 109.1, 30.0 ppm; IR (neat): $\tilde{\nu}=3244$, 1614, 1597, 1572, 1542, 1503, 1463, 1421, 1366, 1346, 1315, 1236, 1165, 1088, 1045, 973, 895, 841, 808, 751, 695, 670, 641, 603, 570 cm^{-1} ; MS (APCI+): m/z : 313.0 $[\text{M}+\text{H}]^+$.

Compound 11d: Yellow solid (166 mg, 80%); $R_f=0.31$ (cyclohexane/EtOAc, 6:4); mp: 199–201 °C; $^1\text{H NMR}$ (300 MHz, CDCl_3): $\delta=12.73$ (s, 1H), 9.34 (s, 1H), 8.09 (dd, 1H, $J_1=8.0$ Hz, $J_2=1.4$ Hz), 7.69 (dd, 1H, $J_1=3.8$ Hz, $J_2=1.1$ Hz), 7.55 (dd, 1H, $J_1=5.0$ Hz, $J_2=1.1$ Hz), 7.48 (ddd, 1H, $J_1=8.6$ Hz, $J_2=7.1$ Hz, $J_3=1.5$ Hz), 7.27–7.19 (m, 2H), 7.09 (dd, 1H, $J_1=5.0$ Hz, $J_2=3.8$ Hz), 3.68 ppm (s, 3H); $^{13}\text{C NMR}$ (75 MHz, CDCl_3): $\delta=161.4$, 159.6, 148.7, 136.8, 136.6, 132.4, 130.5, 130.1, 128.3, 124.8, 122.7, 117.3, 113.8, 109.1, 30.1 ppm; IR (neat): $\tilde{\nu}=3289$, 1646, 1612, 1587, 1536, 1509, 1468, 1417, 1376, 1358, 1315, 1282, 1238, 1164, 1117, 1057, 1046, 995, 972, 890, 853, 837, 820, 774, 754, 716, 698, 652, 592, 578 cm^{-1} ; MS (APCI+): m/z : 301.1 $[\text{M}+\text{H}]^+$.

Compound 11e: Yellow solid (190 mg, 80%); $R_f=0.45$ (cyclohexane/EtOAc, 6:4); mp: 286–288 °C; $^1\text{H NMR}$ (300 MHz, $[\text{D}_6]\text{DMSO}$): $\delta=11.88$ (s, 1H), 11.54 (bs, 1H), 9.67 (s, 1H), 8.05 (dd, 1H, $J_1=8.0$ Hz, $J_2=1.3$ Hz), 7.75–7.65 (m, 2H), 7.57 (d, 1H, $J=8.3$ Hz), 7.51 (dd, 1H, $J_1=7.7$ Hz, $J_2=0.6$ Hz), 7.45 (s, 1H), 7.35 (t, 1H, $J=7.9$ Hz), 7.26 (t, 1H, $J=8.2$ Hz), 7.10 (t, 1H, $J=7.9$ Hz), 3.69 ppm (s, 3H); $^{13}\text{C NMR}$ (75 MHz, $[\text{D}_6]\text{DMSO}$): $\delta=161.1$, 159.6, 152.2, 137.5, 137.0, 130.9, 130.3, 127.0, 124.1, 123.5, 122.0, 121.9, 120.1, 116.0, 114.6, 112.4, 108.5, 105.1, 29.5 ppm; IR (neat): $\tilde{\nu}=3353$, 1647, 1586, 1537, 1417, 1352, 1250, 1094, 791, 739, 646, 571 cm^{-1} ; MS (ESI+): m/z : 356.1 $[\text{M}+\text{Na}]^+$.

Compound 11f: Ochre solid (93 mg, 49%); $R_f=0.54$ (cyclohexane/EtOAc, 5:5); mp: 117–119 °C; $^1\text{H NMR}$ (300 MHz, CDCl_3): $\delta=12.80$ (s, 1H), 8.67 (bs, 1H), 8.03 (dd, 1H, $J_1=8.0$ Hz, $J_2=1.1$ Hz), 7.45 (ddd, 1H, $J_1=8.6$ Hz, $J_2=7.2$ Hz, $J_3=1.5$ Hz), 7.21–7.16 (m, 2H), 3.62 (s, 3H), 2.42 (t, 2H, $J=7.5$ Hz), 1.72 (six, 2H, $J=7.4$ Hz), 0.95 ppm (t, 3H, $J=7.4$ Hz); $^{13}\text{C NMR}$ (75 MHz, CDCl_3): $\delta=173.7$, 159.6, 148.8, 136.6, 130.4, 124.7, 122.6, 117.3, 113.7, 109.2, 38.7, 30.0, 19.3, 13.6 ppm; IR (neat): $\tilde{\nu}=3261$, 2925, 1741, 1639, 1613, 1586, 1566, 1527, 1459, 1407, 1376, 1342, 1313, 1246, 1159, 1094, 1039, 976, 895, 741, 725, 689 cm^{-1} ; MS (APCI+): m/z : 261.2 $[\text{M}+\text{H}]^+$.

Compound 11g: Grey solid (161 mg, 22%); $R_f=0.28$ ($\text{CH}_2\text{Cl}_2/\text{EtOAc}$, 8:2); mp: 311–313 °C; $^1\text{H NMR}$ (300 MHz, $[\text{D}_6]\text{DMSO}$): $\delta=11.75$ (s, 1H), 11.23 (bs, 1H), 9.60 (s, 1H), 7.91 (dd, 1H, $J_1=8.0$ Hz, $J_2=0.8$ Hz), 7.53 (t, 1H, $J=8.3$ Hz), 7.38 (s, 2H), 7.35 (d, 1H, $J=8.1$ Hz), 7.22 (t, 1H, $J=8.0$ Hz), 3.88 (s, 6H), 3.75 ppm (s, 3H); $^{13}\text{C NMR}$ (75 MHz, $[\text{D}_6]\text{DMSO}$): $\delta=166.0$, 160.3, 153.9, 152.6 (2C),

140.6, 136.7, 130.4, 128.4, 123.0, 121.6, 115.4, 115.0, 109.3, 105.6 (2C), 60.1, 56.1 ppm (2C); IR (neat): $\tilde{\nu}=3339$, 2835, 1651, 1611, 1583, 1543, 1503, 1483, 1465, 1433, 1396, 1364, 1335, 1276, 1237, 1192, 1127, 1040, 1001, 930, 893, 856, 812, 755, 731, 669, 652 cm^{-1} ; MS (APCI+): m/z : 370.0 $[\text{M}+\text{H}]^+$.

Compound 11h: Yellow solid (25 mg, 68%); $R_f=0.87$ ($\text{CH}_2\text{Cl}_2/\text{EtOAc}$, 9:1); mp: 196–198 °C; $^1\text{H NMR}$ (300 MHz, CDCl_3): $\delta=13.30$ (s, 1H), 9.34 (s, 1H), 8.09 (d, 1H, $J=8.0$ Hz), 7.70–7.60 (m, 2H), 7.49–7.44 (m, 1H), 7.28–7.16 (m, 2H), 6.78 (dd, 1H, $J_1=9.2$ Hz, $J_2=2.0$ Hz), 3.68 (s, 3H), 2.77 (t, 2H, $J=6.6$ Hz), 1.77 (t, 2H, $J=6.6$ Hz), 1.29 ppm (s, 6H); $^{13}\text{C NMR}$ (75 MHz, CDCl_3): $\delta=166.5$, 159.9, 158.4, 148.7, 136.5, 130.3, 129.7, 127.2, 124.7, 123.2, 122.6, 121.3, 117.8, 117.5, 113.7, 109.5, 75.6, 32.4, 30.0, 26.93 (2C), 22.4 ppm; IR (neat): $\tilde{\nu}=3310$, 2926, 1644, 1607, 1567, 1526, 1484, 1416, 1370, 1352, 1315, 1269, 1234, 1153, 1184, 1120, 1086, 936, 888, 875, 838, 746, 673, 650, 595, 579 cm^{-1} ; MS (ESI+): m/z : 401.0 $[\text{M}+\text{Na}]^+$.

Compound 11i: Yellow solid (38 mg, 78%); $R_f=0.50$ (cyclohexane/EtOAc, 6:4); mp: 180–182 °C; $^1\text{H NMR}$ (400 MHz, CDCl_3): $\delta=13.30$ (s, 1H), 9.44 (s, 1H), 8.19 (dd, 1H, $J_1=8.0$ Hz, $J_2=1.0$ Hz), 7.76 (dd, 1H, $J_1=8.5$ Hz, $J_2=2.2$ Hz), 7.62 (d, 1H, $J=2.2$ Hz), 7.56 (t, 1H, $J=8.4$ Hz), 7.35–7.29 (m, 2H), 6.85 (d, 1H, $J=8.5$ Hz), 6.38 (d, 1H, $J=9.9$ Hz), 5.70 (d, 1H, $J=9.9$ Hz), 3.77 (s, 3H), 1.47 ppm (s, 6H); $^{13}\text{C NMR}$ (100 MHz, CDCl_3): $\delta=166.2$, 159.9, 157.1, 148.8, 136.5, 131.6, 130.3, 129.0, 126.0, 124.7, 124.3, 122.6, 121.4, 121.1, 117.4, 116.6, 113.7, 109.4, 77.6, 30.0, 28.3 ppm (2C); IR (neat): $\tilde{\nu}=3302$, 2925, 1645, 1604, 1529, 1484, 1416, 1373, 1276, 1194, 1166, 1127, 1085, 953, 740, 713, 682, 649, 563 cm^{-1} ; MS (ESI+): m/z : 399.2 $[\text{M}+\text{Na}]^+$.

General protocol for tosylation: Et_3N (2 mmol) was added dropwise to an ice-cooled solution of **11** (1 mmol) in dry CH_2Cl_2 (20 mL) under argon atmosphere. After the mixture stirred for 10 min, *p*-TsCl (1.5 mmol) was added portionwise under argon. After the mixture stirred for 4–12 h at RT, EtOAc was added and the organic layer was washed with aq HCl (1 M), dried over Na_2SO_4 , and concentrated under vacuum. The crude was purified by column chromatography on silica gel to yield 4-tosylquinolones **7a** and **9a–k**.

Compound 7a: Yellow solid (93 mg, 95%); $R_f=0.49$ (CH_2Cl_2); mp: 198–200 °C; $^1\text{H NMR}$ (300 MHz, CDCl_3): $\delta=8.05$ (dd, 1H, $J_1=8.2$ Hz, $J_2=1.2$ Hz), 7.81 (d, 2H, $J=8.4$ Hz), 7.71 (ddd, 1H, $J_1=8.7$ Hz, $J_2=7.3$ Hz, $J_3=1.5$ Hz), 7.45–7.30 (m, 4H), 3.70 (s, 3H), 2.43 (s, 3H); $^{13}\text{C NMR}$ (75 MHz, CDCl_3): $\delta=155.0$, 147.2 (2C), 146.6, 139.3, 134.3, 131.7, 130.3 (2C), 128.6 (2C), 127.0, 123.9, 115.3, 114.7, 30.6, 21.9 ppm; IR (neat): $\tilde{\nu}=1663$, 1597, 1543, 1366, 1182, 1061, 874, 756, 736, 692, 660, 568, 540 cm^{-1} ; MS (APCI+): m/z : 374.9 $[\text{M}+\text{H}]^+$.

Compound 9a: White solid (91 mg, 88%); $R_f=0.39$ ($\text{CH}_2\text{Cl}_2/\text{EtOAc}$, 9:1); mp: 169–171 °C; $^1\text{H NMR}$ (400 MHz, CDCl_3): $\delta=8.14$ (s, 1H), 7.93 (d, 1H, $J=7.8$ Hz), 7.75 (d, 2H, $J=8.2$ Hz), 7.64 (d, 2H, $J=8.7$ Hz), 7.56 (t, 1H, $J=7.5$ Hz), 7.36 (d, 1H, $J=8.5$ Hz), 7.29 (t, 1H, $J=7.6$ Hz), 7.04 (d, 2H, $J=8.1$ Hz), 6.83 (d, 2H, $J=8.7$ Hz), 3.82 (s, 3H), 3.73 (s, 3H), 2.20 ppm (s, 3H); $^{13}\text{C NMR}$ (100 MHz, CDCl_3): $\delta=163.7$, 162.7, 160.4, 145.4, 144.5, 136.8, 134.0, 130.8, 129.8 (4C), 128.0 (2C), 125.4, 124.6, 123.3, 120.0, 118.1, 114.2, 113.5 (2C), 55.5, 30.5, 21.6 ppm; IR (neat): $\tilde{\nu}=1637$, 1599, 1487, 1357, 1252, 1171, 1065, 854, 755, 707, 617, 587, 548, 509 cm^{-1} ; MS (APCI+): m/z : 479.1 $[\text{M}+\text{H}]^+$.

Compound 9b: White solid (50 mg, 88%); $R_f=0.10$ ($\text{CH}_2\text{Cl}_2/\text{EtOAc}$, 9:1); mp: 154–156 °C; $^1\text{H NMR}$ (400 MHz, CDCl_3): $\delta=8.34$ (s, 1H), 7.87 (d, 1H, $J=8.0$ Hz), 7.80 (d, 2H, $J=8.2$ Hz), 7.60 (t, 1H, $J=7.4$ Hz), 7.41 (d, 1H, $J=8.5$ Hz), 7.30 (t, 1H, $J=7.6$ Hz), 7.11 (d, 2H, $J=8.1$ Hz), 7.04 (s, 2H), 3.90 (s, 3H), 3.88 (s, 6H), 3.79 (s, 3H),

2.28 ppm (s, 3H); ^{13}C NMR (100 MHz, CDCl_3): δ = 164.1, 160.6, 153.0 (2C), 145.8, 145.4, 141.6, 137.2, 133.9, 131.2, 129.8 (2C), 128.5, 128.1 (2C), 124.7, 123.4, 120.1, 118.0, 114.3, 105.4 (2C), 61.0, 56.4 (2C), 30.7, 21.6 ppm; IR (neat): $\tilde{\nu}$ = 3276, 1650, 1623, 1596, 1523, 1487, 1416, 1367, 1333, 1230, 1193, 1182, 1122, 1078, 1015, 868, 834, 753, 734, 700, 665, 605, 559 cm^{-1} ; MS (APCI+): m/z : 539.1 $[\text{M}+\text{H}]^+$; Anal. calcd for $\text{C}_{27}\text{H}_{26}\text{N}_2\text{O}_8\text{S}$ (538.12): C 60.21, H 4.87, N 5.20; found: C 59.67, H 4.92, N 5.11.

Compound 9c: Yellow solid (42 mg, 98%); R_f = 0.57 ($\text{CH}_2\text{Cl}_2/\text{EtOAc}$, 9:1); mp: 195–197 °C; ^1H NMR (300 MHz, CDCl_3): δ = 8.13 (s, 1H), 7.82 (dd, 1H, J_2 = 8.1 Hz, J_3 = 1.2 Hz), 7.70 (d, 2H, J = 8.4 Hz), 7.67–7.63 (m, 2H), 7.52 (ddd, 1H, J_1 = 8.6 Hz, J_2 = 7.2 Hz, J_3 = 1.5 Hz), 7.33 (d, 1H, J = 8.4 Hz), 7.23 (t, 1H, J = 8.1 Hz), 7.02 (d, 2H, J = 8.6 Hz), 6.97 (d, 2H, J = 8.7 Hz), 3.70 (s, 3H), 2.18 ppm (s, 3H); ^{13}C NMR (75 MHz, CDCl_3): δ = 166.5 (d, 1C, J_{CF} = 253.1 Hz), 163.2, 160.2, 145.5, 144.9, 136.9, 133.9, 131.0, 130.2 (d, 2C, J_{CF} = 9.0 Hz), 129.7 (2C), 129.2 (d, 1C, J_{CF} = 2.2 Hz), 127.9 (2C), 124.6, 123.3, 119.7, 117.8, 115.3 (d, 2C, J_{CF} = 21.9 Hz), 114.1, 30.5, 21.5 ppm; IR (neat): $\tilde{\nu}$ = 1686, 1644, 1624, 1596, 1487, 1365, 1221, 1193, 1177, 1081, 852, 812, 742, 696, 657, 623, 588 cm^{-1} ; MS (APCI+): m/z : 467.1 $[\text{M}+\text{H}]^+$.

Compound 9d: White solid (223 mg, 95%); R_f = 0.34 ($\text{CH}_2\text{Cl}_2/\text{EtOAc}$, 9:1); mp: 109–111 °C; ^1H NMR (300 MHz, CDCl_3): δ = 8.06 (s, 1H), 8.01 (dd, 1H, J_1 = 8.1 Hz, J_2 = 1.2 Hz), 7.80 (d, 2H, J = 8.3 Hz), 7.62 (ddd, 1H, J_1 = 8.6 Hz, J_2 = 7.3 Hz, J_3 = 1.4 Hz), 7.49 (dd, 1H, J_1 = 5.0 Hz, J_2 = 1.0 Hz), 7.44–7.40 (m, 2H), 7.35 (t, 1H, J = 7.3 Hz), 7.09 (d, 2H, J = 8.1 Hz), 7.04 (dd, 1H, J_1 = 5.0 Hz, J_2 = 3.8 Hz), 3.79 (s, 3H), 2.25 ppm (s, 3H); ^{13}C NMR (75 MHz, CDCl_3): δ = 160.2, 158.6, 145.5, 144.6, 138.0, 136.9, 133.9, 131.3, 131.0, 129.6 (3C), 128.0 (2C), 127.5, 124.8, 123.4, 119.2, 118.1, 114.1, 30.5, 21.6 ppm; IR (neat): $\tilde{\nu}$ = 1645, 1623, 1596, 1496, 1418, 1362, 1277, 1191, 1175, 1078, 850, 815, 758, 734, 700, 655, 604 cm^{-1} ; MS (APCI+): m/z : 455.0 $[\text{M}+\text{H}]^+$.

Compound 9e: White solid (32 mg, 73%); R_f = 0.59 ($\text{CH}_2\text{Cl}_2/\text{EtOAc}$, 8:2); mp: 257–259 °C; ^1H NMR (400 MHz, $[\text{D}_6]\text{DMSO}$): δ = 11.41 (s, 1H), 9.59 (s, 1H), 7.87 (d, 1H, J = 7.9 Hz), 7.76 (td, 1H, J_1 = 8.4 Hz, J_2 = 1.1 Hz), 7.73 (d, 2H, J = 8.4 Hz), 7.69 (d, 1H, J = 8.6 Hz), 7.66 (d, 1H, J = 8.0 Hz), 7.47–7.43 (m, 2H), 7.23 (t, 1H, J = 7.4 Hz), 7.11 (d, 1H, J = 1.1 Hz), 7.08 (t, 1H, J = 7.2 Hz), 7.02 (d, 2H, J = 8.1 Hz), 3.74 (s, 3H), 1.77 ppm (s, 3H); ^{13}C NMR (100 MHz, $[\text{D}_6]\text{DMSO}$): δ = 159.6, 158.9, 147.6, 145.4, 137.4, 136.6, 132.9, 131.5, 130.3, 129.8 (2C), 127.3 (2C), 126.8, 123.8, 123.5, 123.0, 121.8, 120.1, 119.8, 116.7, 115.2, 112.3, 104.9, 30.2, 20.5 ppm; IR (neat): $\tilde{\nu}$ = 3255, 1645, 1626, 1599, 1538, 1366, 1252, 1192, 1177, 1074, 855, 734, 700, 653, 608 cm^{-1} ; MS (APCI+): m/z : 488.1 $[\text{M}+\text{H}]^+$.

Compound 9f: Yellow solid; (28 mg, 70%); R_f = 0.13 (cyclohexane/ EtOAc , 5:5); mp: 163–165 °C; ^1H NMR (300 MHz, CDCl_3): δ = 7.78 (d, 2H, J = 8.3 Hz), 7.65 (dd, 1H, J_1 = 8.1 Hz, J_2 = 0.9 Hz), 7.49 (t, 1H, J = 8.5 Hz), 7.29 (d, 1H, J = 8.6 Hz), 7.28 (d, 2H, J = 8.0 Hz), 7.22 (bs, 1H), 7.16 (t, 1H, J_1 = 8.1 Hz), 3.68 (s, 3H), 2.40 (s, 3H), 2.06 (t, 2H, J = 7.8 Hz), 1.55 (sext, 2H, J = 7.4 Hz), 0.89 ppm (t, 3H, J = 7.4 Hz); ^{13}C NMR (75 MHz, CDCl_3): δ = 170.5, 160.2, 145.8, 144.8, 137.0, 133.9, 130.8, 129.9 (2C), 128.3 (2C), 124.4, 123.0, 119.7, 117.6, 114.0, 38.4, 30.4, 21.7, 18.5, 13.7 ppm; IR (neat): $\tilde{\nu}$ = 3239, 2925, 1681, 1629, 1597, 1499, 1462, 1359, 1289, 1231, 1191, 1173, 1062, 1010, 865, 811, 745, 711, 650, 613, 590, 568, 559 cm^{-1} ; MS (APCI+): m/z : 415.1 $[\text{M}+\text{H}]^+$; Anal. calcd for $\text{C}_{21}\text{H}_{22}\text{N}_2\text{O}_5\text{S}$ (414.19): C 60.85, H 5.35, N 6.76; found: C 60.22, H 5.58, N 6.70.

Compound 9g: The reaction was carried out using a mixture of THF/pyridine (1:1) as solvent to give a beige solid (66 mg, 32%); R_f = 0.44 ($\text{CH}_2\text{Cl}_2/\text{EtOAc}$, 8:2); mp: 218–220 °C; ^1H NMR (300 MHz, $[\text{D}_6]\text{DMSO}$): δ = 12.41 (s, 1H), 9.60 (s, 1H), 7.75 (d, 2H, J = 8.2 Hz),

7.73–7.70 (m, 1H), 7.63 (t, 1H, J = 8.4 Hz), 7.43 (d, 1H, J = 8.1 Hz), 7.33 (t, 1H, J = 8.0 Hz), 7.15 (d, 2H, J = 8.2 Hz), 7.09 (s, 2H), 3.84 (s, 6H), 3.76 (s, 3H), 2.16 ppm (s, 3H); ^{13}C NMR (75 MHz, $[\text{D}_6]\text{DMSO}$): δ = 163.5, 160.0, 152.2 (2C), 148.8, 145.4, 140.3, 136.4, 133.1, 131.1, 129.8 (2C), 127.9, 127.4 (2C), 122.9, 122.6, 121.5, 116.1, 115.4, 105.5 (2C), 60.0, 56.0 (2C), 20.8 ppm; IR (neat): $\tilde{\nu}$ = 2923, 1653, 1579, 1475, 1367, 1333, 1221, 1172, 1125, 1061, 1003, 919, 764, 745, 714, 667, 636, 614 cm^{-1} ; MS (APCI+): m/z : 525.1 $[\text{M}+\text{H}]^+$.

Compound 9h: White solid (66 mg, 79%); R_f = 0.46 ($\text{CH}_2\text{Cl}_2/\text{EtOAc}$, 9:1); mp: 126–128 °C; ^1H NMR (300 MHz, CDCl_3): δ = 7.92 (s, 1H), 7.88 (dd, 1H, J_1 = 8.1 Hz, J_2 = 1.3 Hz), 7.70 (d, 2H, J = 8.3 Hz), 7.50 (ddd, 1H, J_1 = 8.6 Hz, J_2 = 7.3 Hz, J_3 = 1.4 Hz), 7.42 (d, 1H, J = 2.1 Hz), 7.32 (d, 1H, J = 8.5 Hz), 7.31 (d, 1H, J = 8.5 Hz), 7.24 (t, 1H, J = 7.3 Hz), 7.00 (d, 2H, J = 8.3 Hz), 6.66 (d, 1H, J = 8.5 Hz), 3.69 (s, 3H), 2.71 (t, 2H, J = 6.7 Hz), 2.16 (s, 3H), 1.75 (t, 2H, J = 6.7 Hz), 1.28 ppm (s, 6H); ^{13}C NMR (75 MHz, CDCl_3): δ = 163.8, 160.3, 157.6, 145.3, 143.9, 136.6, 134.0, 130.6, 129.8, 129.7 (2C), 128.0 (2C), 127.2, 124.6, 124.3, 123.2, 120.6, 120.0, 118.2, 117.0, 114.0, 75.3, 32.5, 30.5, 26.9 (2C), 22.3, 21.6 ppm; IR (neat): $\tilde{\nu}$ = 3265, 1646, 1628, 1603, 1482, 1364, 1320, 1256, 1236, 1194, 1180, 1152, 1119, 1078, 1016, 949, 911, 866, 839, 814, 732, 700, 660, 608, 561 cm^{-1} ; MS (APCI+): m/z : 533.1 $[\text{M}+\text{H}]^+$.

Compound 9i: Yellow oil (19 mg, 87%); R_f = 0.59 ($\text{CH}_2\text{Cl}_2/\text{EtOAc}$, 8:2); ^1H NMR (300 MHz, CDCl_3): δ = 7.92 (d, 1H, J = 1.1 Hz), 7.90 (s, 1H), 7.69 (d, 2H, J = 8.3 Hz), 7.53 (t, 1H, J = 8.4 Hz), 7.38–7.24 (m, 4H), 7.00 (d, 2H, J = 8.4 Hz), 6.66 (d, 1H, J = 8.4 Hz), 6.25 (d, 1H, J = 9.9 Hz), 5.61 (d, 1H, J = 9.9 Hz), 3.71 (s, 3H), 2.17 (s, 3H), 1.40 (s, 6H); ^{13}C NMR (75 MHz, CDCl_3): δ = 163.5, 160.3, 156.5, 145.4, 143.9, 136.6, 134.0, 131.3, 130.7, 129.7 (2C), 129.1, 128.0 (2C), 126.3, 125.3, 124.6, 123.3, 121.6, 120.6, 119.8, 118.2, 116.0, 114.1, 77.4, 30.5, 28.3 (2C), 21.6 ppm; IR (neat): $\tilde{\nu}$ = 3249, 2975, 1643, 1600, 1575, 1478, 1361, 1317, 1268, 1213, 1190, 1177, 1122, 1075, 1013, 960, 912, 870, 814, 741, 697, 671, 659, 636, 621, 608, 595, 584, 578 cm^{-1} ; MS (APCI+): m/z : 531.1 $[\text{M}+\text{H}]^+$.

Compound 9j: The reaction was carried out using pyridine as solvent to afford compound **9j** without purification from **3b** as a yellow solid (20 mg, 15% over three steps); R_f = 0.25 ($\text{CH}_2\text{Cl}_2/\text{EtOAc}$, 5:5); mp: 214–216 °C; ^1H NMR (300 MHz, $[\text{D}_6]\text{DMSO}$): δ = 12.21 (s, 1H), 9.16 (s, 1H), 7.74 (d, 2H, J = 8.3 Hz), 7.59 (d, 1H, J = 9.0 Hz), 7.53 (d, 1H, J = 2.1 Hz), 7.43 (dd, 1H, J_1 = 8.6 Hz, J_2 = 2.1 Hz), 7.18 (d, 2H, J = 8.3 Hz), 6.95 (dd, 1H, J_1 = 9.0 Hz, J_2 = 2.4 Hz), 6.89 (d, 1H, J = 2.4 Hz), 6.69 (d, 1H, J = 8.6 Hz), 3.85 (s, 3H), 2.78 (t, 2H, J = 6.5 Hz), 2.18 (s, 3H), 1.82 (t, 2H, J = 6.5 Hz), 1.32 ppm (s, 6H); ^{13}C NMR (75 MHz, $[\text{D}_6]\text{DMSO}$): δ = 163.9, 161.4, 160.4, 156.4, 149.0, 145.2, 138.2, 133.0, 129.8 (3C), 127.4, (2C), 127.1, 124.5, 124.1, 119.9, 118.8, 115.9, 111.6, 109.9, 98.0, 74.9, 55.5, 31.9, 26.5 (2C), 21.7, 20.9 ppm; IR (neat): $\tilde{\nu}$ = 1655, 1516, 1482, 1358, 1259, 1175, 1119, 1061, 946, 837, 736, 675 cm^{-1} ; MS (APCI+): m/z : 549.0 $[\text{M}+\text{H}]^+$.

Compound 9k: White solid (40 mg, 96%); R_f = 0.27 ($\text{CH}_2\text{Cl}_2/\text{EtOAc}$, 8:2); mp: 144–146 °C; ^1H NMR (300 MHz, CDCl_3): δ = 8.34 (s, 1H), 7.78 (dd, 1H, J_1 = 8.1 Hz, J_2 = 1.0 Hz), 7.73 (dd, 1H, J_1 = 3.8 Hz, J_2 = 1.2 Hz), 7.61–7.56 (m, 2H), 7.41 (d, 1H, J = 8.4 Hz), 7.27 (t, 1H, J = 7.6 Hz), 7.13 (s, 2H), 6.97 (dd, 1H, J_1 = 4.9 Hz, J_2 = 4.0 Hz), 3.91 (s, 3H), 3.90 (s, 6H), 3.79 ppm (s, 3H); ^{13}C NMR (75 MHz, CDCl_3): δ = 164.3, 160.2, 153.0 (2C), 144.4, 141.5, 137.0, 135.6, 135.5, 134.9, 131.0, 128.6, 127.7, 124.2, 123.2, 120.4, 117.4, 114.2, 105.2 (2C), 61.0, 56.3 (2C), 30.6 ppm; IR (neat): $\tilde{\nu}$ = 3268, 1641, 1621, 1596, 1486, 1415, 1363, 1333, 1287, 1223, 1180, 1126, 1097, 1073, 1005, 920, 864, 827, 753, 727, 698, 669, 610, 584 cm^{-1} ; MS (APCI+): m/z : 531.0 $[\text{M}+\text{H}]^+$.

Biology

Cell culture and drug treatment: MCF-7 (ER-positive) and MDA-MB-231 (ER-negative) cells were grown in Dulbecco's modified eagle medium (DMEM, Lonza, Vervier, Belgium) supplemented with L-glutamine (2 mM), penicillin (5 IU mL⁻¹), streptomycin (50 IU mL⁻¹), 10% fetal calf serum (FCS), charcoal Norit A (1%), and Dextran T70 (0.1%) for 30 min at room temperature. The monosodium novobiocin salt was obtained from Sigma-Aldrich (St. Louis, MO, USA) and proteasome inhibitor MG132 from Calbiochem (La Jolla, CA, USA). Nvb was diluted in water, and coumarin analogues (10 mM stock solutions) were diluted in DMSO. Drug treatments of cells were performed over various time periods in the presence or absence of MG132 (5 μM).

Quantification of cell survival/proliferation: Cells were seeded in 96-well plates at 5000 cells per well and, after 24 h, serial dilutions of drugs were added. After 72 h, 500 μg mL⁻¹ of 3-(4,5-dimethylthiazol-2-yl)-2,5-diphenyltetrazolium bromide (MTT, Sigma-Aldrich) was added to each well over 3 h at 37 °C. Medium was removed, and MTT formazan crystals were dissolved in 100 μL DMSO, followed by gentle agitation for 10 min. The absorbance of converted dye, which directly correlates to the number of viable cells, was measured at 570 nm with background subtraction at 650 nm using a spectrophotometric microtiter reader (Metertech, Σ960, Fisher-Bio-block, Illkirch, France). All determinations were carried out in sextuplicate, with each experiment repeated three times. The percentage of survival was calculated as the absorbance ratio of treated to untreated cells. IC₅₀ values were determined as the drug concentrations able to inhibit cell growth by 50%, as compared with growth of vehicle-treated cells.

Cell extracts and Western blots: Cells were grown to 50% confluence in 60 mm dishes before exposure to various agents as indicated in the text and figure legends. Cells were rinsed in phosphate-buffered saline (PBS), scraped into PBS, collected by centrifugation, resuspended in ice-cold lysis buffer (50 mM Tris-HCl (pH 7.5), 150 mM NaCl, 1 mM EGTA, 10% (v/v) glycerol, 1% Triton X-100, 1.5 mM MgCl₂, 10 mM NaF, 10 mM sodium pyrophosphate, and 1 mM Na₃VO₄) containing protease inhibitors (Complete reagent, Roche Diagnostics, Indianapolis, IN), and kept on ice for 15 min with occasional vortexing. Insoluble debris were removed by centrifugation at 15 000 g for 5 min at 4 °C, and cell lysates were boiled in Laemmli sample buffer for 3 min. TCEs were obtained from pelleted cells by resuspension in lysis buffer for 30 min at 4 °C and boiling for 5 min in Laemmli sample buffer. Protein concentration was determined using the Bio-Rad Assay. Equal amounts of protein (20 μg) were fractionated by 8% or 12% SDS-polyacrylamide gel electrophoresis (SDS-PAGE) and transferred onto Immobilon-P membranes (Millipore, Saint Quentin en Yvelines, France). Membranes were blocked for 1 h at 37 °C with 10% dry nonfat milk in PBS containing 0.1% Tween20. ER was detected with the D12 (ER epitope: amino acids 2–185) mouse monoclonal anti-ER antibody (Santa Cruz, CA, USA) at 1 μg mL⁻¹ in PBST/2% milk overnight at 4 °C. Antigen/antibody complexes were detected by incubation with a biotinylated anti-mouse antibody, followed by revelation with the avidin/peroxidase complex (Vectastain ABC Elite Kit, Vector Laboratories, Inc., Burlingame, CA). p23 was probed with a biotinylated anti-mouse antibody, followed by revelation with the avidin-peroxidase complex. Other primary antibodies, for HER2 (C-18), Raf-1 (C-12), Cdk4 (C22), and PARP (F-2), were from Santa Cruz and used at 1 μg mL⁻¹. The JJ3 monoclonal antibody against p23 was a generous gift from D.O. Toft (Mayo Clinic, Rochester, MN). The antigen/antibody complexes were detected with appropriate secondary horseradish peroxidase-conjugated antibodies (Santa

Cruz). Blots were developed using the Immobilon Western Detection Reagent (Millipore). Depending on mobility of the proteins, membranes were either stripped (1 h at 50 °C in a medium containing 62.5 mM Tris-HCl pH 6.8, 2% SDS, and 100 mM 2-mercaptoethanol) or extensively washed before reprobing with different primary antibodies. Equal protein loading was assessed by examination of the intensities of nonspecific (NS) signals elicited by the commercial antibodies used that were unresponsive to treatments. **Flow cytometry analysis:** Cells (1.3 × 10⁵ cells mL⁻¹) were cultured in the presence or absence of novobiocin analogues at 100 μM. Nvb at the same concentration served as a reference inhibitor. After treatment for 48 and 72 h, cells were washed and fixed in PBS/EtOH (30:70). For cytofluorometric examination, cells (10⁴) were incubated for 30 min in 0.2% PBS/Triton X100, 1 mM EDTA, and 50 μg mL⁻¹ propidium iodide (PI) in PBS, supplemented by RNase (0.5 mg mL⁻¹). The number of cells in the different phases of the cell cycle was determined, and the percentage of apoptotic cells was quantified. Analyses were performed with a FACS Calibur (Becton Dickinson, Le Pont de Claix, France). Cell Quest software was used for data acquisition and analysis.

Acknowledgements

The CNRS is gratefully acknowledged for financial support of this research. We thank the European Union (EU) within the EST network BIOMEDCHEM (MEST-CT-2005-020580) for a Ph.D. grant to D. A., a fellowship to L. C., and for financial support. Region Ile-de-France is also acknowledged for support. Thanks also to E. Morvan for her help in the NMR experiments and A. Solgadi for performing MS analysis (SAMM platform, Châtenay-Malabry).

Keywords: antiproliferative agents • apoptosis • Hsp90 inhibitors • novobiocin • quinolein-2-ones

- [1] a) Y. L. Janin, *J. Med. Chem.* **2005**, *48*, 7503–7512; b) M. Sgobba, G. Rastelli, *ChemMedChem* **2009**, *4*, 1399–1409; c) S. Messaoudi, J.-F. Peyrat, J.-D. Brion, M. Alami, *Anticancer Agents Med. Chem.* **2008**, *8*, 761–782; d) J. F. Peyrat, S. Messaoudi, J. D. Brion, M. Alami, *Atlas Genet. Cytogenet. Oncol. Haematol.* April **2010**; <http://AtlasGeneticsOncology.org/Deep/HSP90inCancerTreatmentID20086.html> e) Y. L. Janin, *Drug Discovery Today* **2010**, *15*, 342–353.
- [2] a) L. Neckers, *J. Biosci.* **2007**, *32*, 517–530; b) M. W. Amolins, B. S. J. Blagg, *Mini-Rev. Med. Chem.* **2009**, *9*, 140–152.
- [3] a) A.; Maloney, P. Workman, *Expert Opin. Biol. Ther.* **2002**, *2*, 3–24; b) L. Whitesell, S.-L. Lindquist, *Nat. Rev. Cancer* **2005**, *5*, 761–772.
- [4] a) H. Zhang, F. Burrows, *J. Mol. Med.* **2004**, *82*, 488–499; b) B. S. J. Blagg, T. D. Kerr, *Med. Res. Rev.* **2006**, *26*, 310–338.
- [5] S. Sharp, P. Workman, *Adv. Cancer Res.* **2006**, *95*, 323–348.
- [6] a) T. Taldone, A. Gozman, R. Maharaj, G. Chiosis, *Curr. Opin. Pharmacol.* **2008**, *8*, 370–374; b) C. E. Stebbins, A. A. Russo, C. Schneider, N. Rosen, F. U. Hartl, N. P. Pavletich, *Cell* **1997**, *89*, 239–250; c) J. P. Grenert, W. P. Sullivan, P. Fadden, T. A. Haystead, J. Clark, E. Mimnaugh, H. Krutzsch, H. J. Ochel, T. W. Schulte, E. Sausville, L. M. Neckers, D. O. Toft, *J. Biol. Chem.* **1997**, *272*, 23843–23850; d) L. Whitesell, E. G. Mimnaugh, B. De Costa, C. E. Myers, L. M. Neckers, *Proc. Natl. Acad. Sci. USA* **1994**, *91*, 8324–8328; e) P. Workman, F. Burrows, L. Neckers, N. Rosen, *Ann. NY Acad. Sci.* **2007**, *1113*, 202–216; f) B. Felding-Habermann, *Clin. Exp. Metastasis* **2003**, *21*, 203–213; g) M. A. Biamonte, R. Van de Water, J. W. Arndt, R. H. Scannevin, D. Perret, W.-C. J. Lee, *Med. Chem.* **2010**, *53*, 3–17.
- [7] a) M. G.; Marcu, A. Chadli, I. Bohouche, B. Catelli, L. M. Neckers, *J. Biol. Chem.* **2000**, *275*, 37181–37186; Marcu, T. W. Schulte, L. Neckers, *Natl. Cancer Inst. Monogr.* **2000**, *92*, 242–248; b) M. G.; Marcu, A. Chadli, I. Bohouche, B. Catelli, L. M. Neckers, *J. Biol. Chem.* **2000**, *275*, 37181–37186;

- c) R. K. Allan, D. Mok, B. K. Ward, T. Ratajczak, *J. Biol. Chem.* **2006**, *281*, 7161–7171.
- [8] B. G. Yun, W. Huang, N. Leach, S. D. Hartson, R. L. Matts, *Biochemistry* **2004**, *43*, 8217–8229.
- [9] a) G. Le Bras, C. Radanyi, J.-F. Peyrat, J.-D. Brion, M. Alami, V. Marsaud, B. Stella, J.-M. Renoir, *J. Med. Chem.* **2007**, *50*, 6189–6200; b) C. Radanyi, G. Le Bras, S. Messaoudi, C. Bouclier, J.-F. Peyrat, J.-D. Brion, V. Marsaud, J.-M. Renoir, M. Alami, *Bioorg. Med. Chem. Lett.* **2008**, *18*, 2495–2498.
- [10] C. Radanyi, G. Le Bras, V. Marsaud, J.-F. Peyrat, S. Messaoudi, M. G. Catelli, J.-D. Brion, M. Alami, J.-M. Renoir, *Cancer Lett.* **2009**, *274*, 88–94.
- [11] C. Radanyi, G. Le Bras, C. Bouclier, S. Messaoudi, J.-F. Peyrat, J.-D. Brion, M. Alami, J.-M. Renoir, *Biochem. Biophys. Res. Commun.* **2009**, *379*, 514–518.
- [12] a) S. Sahnoun, S. Messaoudi, J.-F. Peyrat, J.-D. Brion, M. Alami, *Tetrahedron Lett.* **2008**, *49*, 7279–7283; b) S. Sahnoun, S. Messaoudi, J.-D. Brion, M. Alami, *Org. Biomol. Chem.* **2009**, *7*, 4271–4278; c) S. Sahnoun, S. Messaoudi, J.-B. Brion, M. Alami, *Eur. J. Org. Chem.* **2010**, 6097–6102; d) S. Messaoudi, J.-B. Brion, M. Alami, *Adv. Synth. Catal.* **2010**, *352*, 1677–1687.
- [13] a) P. R. Angibaud, G. C. Sanz, M. G. Venet, P. Muller, *Janssen Pharmaceutica NV*, EP 1 162 201, **2001**; b) C. A. Hicks, M. A. Ward, N. Ragumoorthy, S. J. Ambler, C. P. Dell, D. Dobson, M. J. O'Neill, *Brain Res.* **1999**, *819*, 65–74; c) W. W. K. R. Mederski, M. Osswald, D. Dorsch, M. Christadler, C.-J. Schmitges, C. Wilm, *Bioorg. Med. Chem. Lett.* **1997**, *7*, 1883–1886; d) P. Hewawasam, N. Chen, M. Ding, J. T. Natale, C. G. Boissard, S. Yeola, V. K. Gribkoff, J. Starrett, S. I. Dworetzky, *Bioorg. Med. Chem. Lett.* **2004**, *14*, 1615–1618; e) P. Hewawasam, W. Fan, M. Ding, K. Flint, D. Cook, G. D. Goggings, R. A. Myers, V. K. Gribkoff, C. G. Boissard, S. I. Dworetzky, J. E. Starret, N. J. Lodge, *J. Med. Chem.* **2003**, *46*, 2819–2822; f) P. Hewawasam, W. Fan, J. Knipe, S. L. Moon, V. C. G. Boissard, K. Gribkoff, J. E. Starret, *Bioorg. Med. Chem. Lett.* **2002**, *12*, 1779–1783; g) K. H. Raitio, J. R. Savinainen, J. Vepsäläinen, J. T. Laitinen, A. Poso, T. Järvinen, T. Nevalainen, *J. Med. Chem.* **2006**, *49*, 2022–2027; h) A. A. Cordi, P. Desos, J. C. R. Randle, J. Lepagnol, *Bioorg. Med. Chem.* **1995**, *3*, 129–141; i) P. Desos, J. M. Lepagnol, P. Morain, P. Lestage, A. A. Cordi, *J. Med. Chem.* **1996**, *39*, 197–206; j) R. W. Carling, P. D. Leeson, K. W. Moore, J. D. Smith, C. R. Moyes, I. M. Mawer, S. Thomas, T. Chan, R. Baker, A. Foster, S. Grimwood, J. A. Kemp, G. R. Marshall, M. D. Tricklebank, K. L. Saywell, *J. Med. Chem.* **1993**, *36*, 3397–3408.
- [14] a) D. Audisio, S. Messaoudi, J.-F. Peyrat, J.-D. Brion, M. Alami, *Tetrahedron Lett.* **2007**, *48*, 6928–6932; b) S. Messaoudi, D. Audisio, J.-D. Brion, M. Alami, *Tetrahedron* **2007**, *63*, 10202–10210.
- [15] a) D. R. Buckle, B. C. C. Cantello, H. Smith, B. A. Spicer, *J. Med. Chem.* **1975**, *18*, 726–732; b) S. X. Cai, Z. L. Zhou, J. C. Huang, E. R. Whittemore, Z. O. Egbuwokwu, J. E. Hawkinson, R. M. Woodward, E. Weber, J. F. Keana, *J. Med. Chem.* **1996**, *39*, 4682–4686.
- [16] Z. Hu, X. Jiang, W. Han, *Tetrahedron Lett.* **2008**, *49*, 5192–5195.
- [17] a) F. R. Calabri, V. Colotta, D. Catarzi, F. Varano, O. Lenzi, G. Filacchioni, C. Costagli, A. Galli, *Eur. J. Med. Chem.* **2005**, *40*, 897–907; b) W. Steinschifter, W. Fiala, W. Stadlbauer, *J. Heterocycl. Chem.* **1994**, *31*, 1647–1652.
- [18] A. J. Caplan, A. K. Mandal, M. A. Theodoraki, *Trends Cell Biol.* **2007**, *17*, 87–92.
- [19] a) T. Zhang, A. Hamza, X. Cao, B. Wang, S. Yu, C. G. Zhan, D. Sun, *Mol. Cancer Ther.* **2008**, *7*, 162–170; b) A. Chadli, S. J. Felts, Q. Wang, W. P. Sullivan, M. V. Botuyan, A. Fauq, M. Ramirez-Alvarado, G. Mer, *J. Biol. Chem.* **2009**, *285*, 4224–4231; c) K. Eckert, J.-M. Saliou, L. Monlezun, A. Vigouroux, N. Atmane, C. Caillat, S. Quevillon-Chérueil, K. Madiona, M. Nicaise, S. Lazereg, A. Van Dorselaer, S. Sanglier-Cianféroni, P. Meyer, S. Moréra, *J. Biol. Chem.* **2010**, *285*, 31304–313012.
- [20] S. B. Bratton, M. MacFarlane, K. Cain, G. M. Cohen, *Exp. Cell Res.* **2000**, *256*, 27–33.
- [21] R. U. Jänicke, M. L. Sprengart, M. R. Wati, A. G. Porter, *J. Biol. Chem.* **1998**, *273*, 9357–9360.
- [22] Y. Liang, C. Yan, N. F. Schor, *Oncogene* **2001**, *20*, 6570–6578.
- [23] a) J. Mollerup, T. N. Krogh, P. F. Nielsen, M. W. Berchtold, *FEBS Lett.* **2003**, *555*, 478–482; b) G. Gausdal, B. T. Gjertsen, K. E. Fladmark, H. Demol, J. Vandekerckhove and S.-O. Døskeland, *Leukemia* **2004**, *18*, 1989–1996; c) J. Mollerup, M. W. Berchtold, *FEBS Lett.* **2005**, *579*, 4187–4192.
- [24] F. Forafonov, O. A. Toogun, I. Grad, E. Suslova, B. C. Freeman, D. Picard, *Moll. Cell Biol.* **2008**, *28*, 3446–3456.
- [25] J. W. Shay, S. Bacchetti, *Eur. J. Cancer* **1997**, *33*, 787–791.
- [26] L. Yu, A. Alva, H. Su, P. Dutt, E. Freundt, S. Welsh, E. H. Baehrecke, M. J. Lenardo, *Science* **2004**, *304*, 1500–1502.
- [27] a) F. Reggiori, D. J. Klionsky, *Eukaryotic Cell* **2002**, *1*, 11–21; b) T. Shintani, D. I. J. Klionsky, *Science* **2004**, *306*, 990–995.

Received: November 16, 2010

Revised: January 18, 2011

Published online on March 4, 2011